THE JOURNAL OF PHYSICAL CHEMISTRY B

Article

pubs.acs.org/JPCB

Impact of Self-Aggregation on the Formation of Ionic-Liquid-Based Aqueous Biphasic Systems

Mara G. Freire,*[,†,‡] Catarina M. S. S. Neves,[‡] José N. Canongia Lopes,[†,§] Isabel M. Marrucho,[†,‡] João A. P. Coutinho,[‡] and Luís Paulo N. Rebelo*[,†]

[†]Instituto de Tecnologia Química e Biológica, Universidade Nova de Lisboa (www.itqb.unl.pt), Av. República, 2780-901 Oeiras, Portugal

[‡]Departamento de Química, CICECO (www.ciceco.ua.pt), Universidade de Aveiro, 3810-193 Aveiro, Portugal

[§]Centro de Química Estrutural, Instituto Superior Técnico (cqe.ist.utl.pt), 1049-001 Lisboa, Portugal

Supporting Information

ABSTRACT: This work reports on the systematic investigation of the influence of the cation alkyl side-chain length of 1-alkyl-3-methylimidazolium chloride ionic liquids ([$C_nC_1$im]Cl, with n = 1−14), as well as the substitution of the most acidic hydrogen in the imidazolium core by a methyl group, in the formation of aqueous biphasic systems. Ternary phase diagrams, tie-lines, tie-line slopes, tie-line lengths, and critical points for the several systems (ionic liquid + water + K_3PO_4) were determined and reported at 298 K and atmospheric pressure. It is shown that the increase of the cation alkyl chain length enhances the formation of aqueous biphasic systems if alkyl chain lengths until the hexyl are considered. The results for longer alkyl side chains show, nevertheless, that the phenomenon is more complex than previously admitted and that the capacity of the ionic liquid to self-aggregate also governs its ability to phase separate. The effect of the alkyl side-chain length on the phase-forming ability of the studied systems was quantitatively evaluated based on their salting-out coefficients derived from a Setschenow-type behavior. The aptitude of each ionic liquid for liquid−liquid demixing as a function of the cation alkyl side-chain length clearly follows three different patterns. The results obtained for the trisubstituted cation indicate that the hydrogen-bonding interactions between the ionic liquid cation and water are not a relevant issue in the formation of aqueous two-phase systems. In general, for the [$C_nC_1$im]Cl series, a multifaceted ratio between entropic contributions and the ability of each ionic liquid to self-aggregate in aqueous media control the phase behavior.

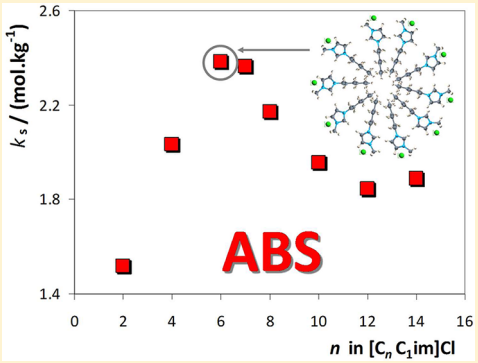

INTRODUCTION

Typical aqueous biphasic systems (ABS) consist of two immiscible aqueous-rich phases based on polymer/polymer, polymer/salt, or salt/salt combinations.[1] In the latter example, at least one of the salts is usually an ionic surfactant. Classic polymer-based ABS have been largely explored.[1,2] Yet, in recent years, ionic liquids (ILs), a class of salt-like materials with melting temperatures below 373 K, have been suggested as feasible alternatives to polymeric-rich phases.[3−19] Both the combination of ILs with salting-out-inducing salts[3−13] as well as those with weaker salting-out species such as carbohydrates[14−16] and amino acids[17,18] have proven to undergo liquid−liquid demixing in aqueous solutions. Moreover, recent advances have shown that anionic surfactants are also able to form IL-based ABS.[19] Substituting polymers with ILs has some significant advantages because most of the polymer-based ABS have high viscosities and display a slow phase separation, drawbacks generally avoided with IL-based ABS. A review regarding IL-based ABS and their potential applications was recently published, and it provides a complete compilation of the data published hitherto and also highlights the advantages of these new systems.[20]

Besides the negligible volatility and nonflammability of ILs,[21,22] one of the main advantages of IL-based ABS is the ability to tailor their phases' polarities by the targeted manipulation of the cation/anion arrangement aiming at performing specific extractions. When dealing with polymers, usually hydrophobic compounds, the tailoring of the properties of the coexisting phases to improve particular extractions is more complex and is mainly achieved by the polymer functionalization.[23] In addition to the large array of combinations between cations and anions that can be utilized, the tuning of the ILs' phases is also possible due to the fact that, unlike most traditional molecular solvents, ILs can be regarded as nanosegregated media, composed of a polar network permeated by nonpolar domains.[24−26] These different regions are kept separate by the different types of interactions

Received: November 18, 2011
Revised: June 1, 2012
Published: June 8, 2012

ACS Publications © 2012 American Chemical Society

prevailing in each of them (strong electrostatic interactions dominate the polar network whereas van der Waals dispersion forces control the nonpolar domains). This dual nature allows ILs to interact selectively with different types of solutes/solvents and to present distinct phase behavior. The inherent amphiphilic nature of long-chained IL cations also remains outside of their pure state, and in aqueous solutions, their aggregation phenomenon is a significant issue that leads to the formation of micelles with specific structures, shapes, and properties.[27] Hence, it is expected that this fact may be responsible for the unique solution properties of ILs, including their capacity to form ABS.

Najdanovic-Visak et al.[5] reported the pioneer temperature−composition pseudobinary systems for K_3PO_4, water, and chloride ILs combined with the cations 1-butyl-3-methylimidazolium, 1-methyl-3-octylimidazolium, and 1-decyl-3-methylimidazolium. The authors[5] postulated that the locus of the homogeneous region increases as the alkyl side chain increases, which might be a direct consequence of the self-aggregation of the longer-chain ionic fluids in aqueous media. Subsequently, we observed[8] that for a common inorganic salt, ABS are favorably formed by ILs with longer aliphatic chains at the imidazolium core, a direct result of the increase of the fluid hydrophobicity and lower affinity for water. In this previous work,[8] the series studied was that of 1-alkyl-3-methylimidazolium chloride ILs, $[C_nC_1im]Cl$, whereas $n = 6$ was the longest alkyl chain studied. Therefore, opposite patterns had previously been identified,[5,8] largely depending on the cation alkyl side-chain length or on the series of ILs investigated. Moreover, Deng et al.[28] reported IL-based ABS composed of different inorganic salts, water, and $[C_nC_1im]Cl$ (n = 4, 6, and 8), whereas Pei et al.[29,30] presented the rank of bromide ILs of the type $[C_nC_1im]Br$ (n = 4, 6, 8, and 10). In fact, both groups[28−30] detected an anomalous behavior regarding the ILs' ability to form ABS (after $n = 6$), although no major conclusions were provided.

This work aims at providing new insights into the main mechanisms that control the formation of IL-based ABS, with particular emphasis on an extended analysis of the effect of the cation alkyl side-chain length. To this end, we investigated the liquid−liquid phase behavior of ternary systems composed of 1-alkyl-3-methylimidazolium chloride ILs (from methyl to tetradecyl), water, and K_3PO_4. The effect of the substitution of the most acidic hydrogen at the imidazolium core by a methyl group also complemented the study. Changing the IL anion or cation nature is an effective way to manipulate the hydrogen-bonding character of the IL, while increasing the cation alkyl chain length can alter their dispersive interactions. Within this focus and aiming at developing a general picture of the phenomena occurring in IL-based ABS, particularly at the molecular level, several approaches and comparisons were used to support the experimental phase diagrams obtained. The Setschenow salting-out coefficients were used as a quantitative measure of the two-phase forming ability because, in this case, they reflect the extent of the preferential hydration of each IL.

EXPERIMENTAL SECTION

Materials. The following ILs were studied to determine the corresponding phase diagrams: 1,3-dimethylimidazolium chloride, $[C_1C_1im]Cl$; 1-ethyl-3-methylimidazolium chloride, $[C_2C_1im]Cl$; 1-butyl-3-methylimidazolium chloride, $[C_4C_1im]Cl$; 1-hexyl-3-methylimidazolium chloride, $[C_6C_1im]Cl$; 1-heptyl-3-methylimidazolium chloride, $[C_7C_1im]Cl$; 1-methyl-3-octylimidazolium chloride, $[C_8C_1im]Cl$; 1-decyl-3-methylimidazolium chloride, $[C_{10}C_1im]Cl$; 1-dodecyl-3-methylimidazolium chloride, $[C_{12}C_1im]Cl$; 1-methyl-3-tetradecylimidazolium chloride, $[C_{14}C_1im]Cl$; and 1-butyl-2,3-dimethylimidazolium chloride, $[C_4C_1C_1im]Cl$. All ILs were purchased from Iolitec. To reduce the volatile impurities in the ILs, individual samples were dried under constant agitation at vacuum and moderate temperature (343 K) for a minimum of 48 h. After this step, the purity of each IL was further checked by ^1H and ^{13}C NMR spectra (purity > 99 wt % for all samples). Sketches of the general ionic structures of the fluids studied appear in Figure 1.

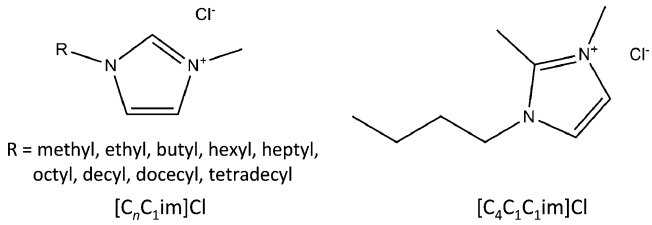

Figure 1. Ionic structures of the studied ILs.

The inorganic salt K_3PO_4 was acquired from Sigma (purity >98 wt %). The water employed was double distilled, passed through a reverse osmosis system, and further treated with a Milli-Q plus 185 water purification equipment.

EXPERIMENTAL PROCEDURE

Phase Diagrams and Tie-Lines. The ternary liquid−liquid phase diagrams were determined by the cloud point titration method at (298 ± 1) K and atmospheric pressure. Aqueous solutions of K_3PO_4 at ~40 wt % and aqueous solutions of the diverse hydrophilic ILs at ~60 wt % were prepared and used for the determination of the binodal boundaries. The experimental procedure consists of two major steps: (i) the dropwise addition of the aqueous inorganic salt solution to each IL aqueous solution until a cloudy and biphasic solution is detected and (ii) the dropwise addition of ultrapure water until a clear, limpid solution corresponding to the monophasic regime forms. All of the procedure was carried out under constant stirring. The ternary systems' compositions were determined by weight quantification of all components within $\pm 10^{-4}$ g.

The experimental binodal curves were fitted by least-squares regression according to eq 1.[31]

$$[IL] = A \exp[(B \times [K_3PO_4]^{0.5}) - (C \times [K_3PO_4]^3)] \quad (1)$$

where [IL] and $[K_3PO_4]$ are the IL and the inorganic salt weight fraction percentages, respectively, and A, B, and C are fitted constants obtained by the regression of the experimental data.

Tie-lines (TLs) were assessed by a gravimetric method originally proposed by Merchuck et al.[31] and making use of the fitting of the binodal data by eq 1. A ternary mixture composed of K_3PO_4 + water + IL at the biphasic region was gravimetrically prepared within $\pm 10^{-4}$ g, vigorously stirred, and left to equilibrate for at least 12 h at 298 K, aiming at a complete separation of the coexisting aqueous phases. In this step, small ampules (10 cm^3) were used to facilitate the separation of the phases. The phases were further separated and individually weighed within $\pm 10^{-4}$ g. Each TL was determined through the relationship between the top phase and the overall

dx.doi.org/10.1021/jp211132z | J. Phys. Chem. B 2012, 116, 7660−7668

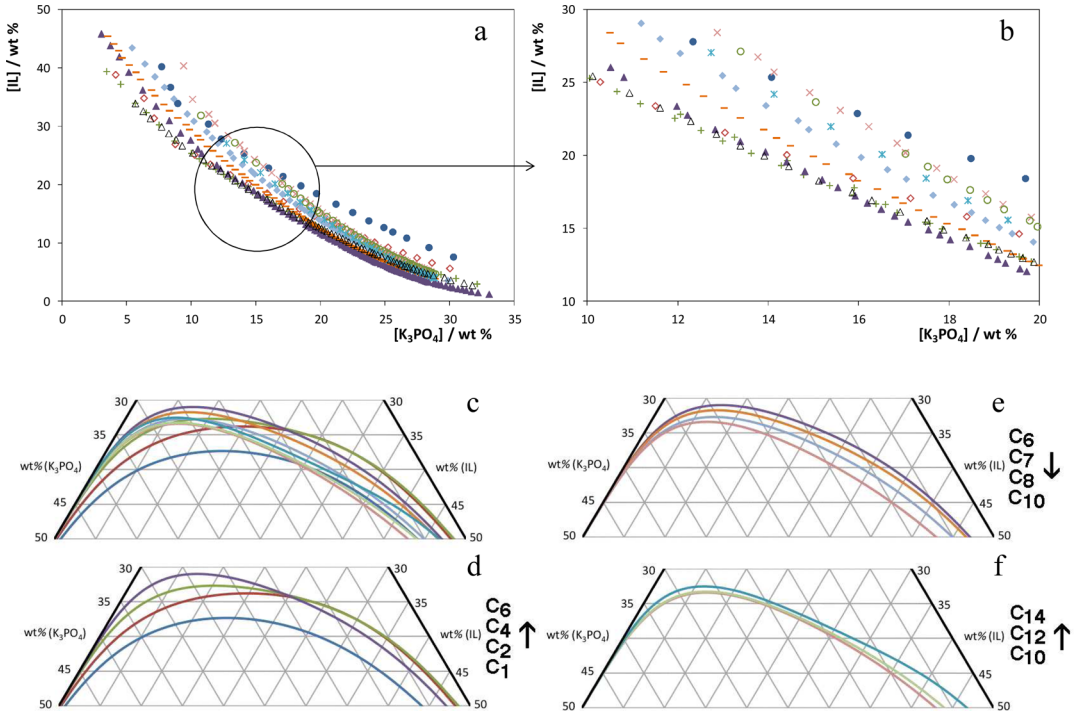

Figure 2. Ternary phase diagrams for K_3PO_4 + water + chloride-based ILs at 298 K and atmospheric pressure. (Top) Experimental data points in an orthogonal diagram (weight fraction units): ●, $[C_1C_1im]Cl$; ◊, $[C_2C_1im]Cl$; +, $[C_4C_1im]Cl$; ▲, $[C_6C_1im]Cl$; -, $[C_7C_1im]Cl$; ♦, $[C_8C_1im]Cl$; ×, $[C_{10}C_1im]Cl$; ○, $[C_{12}C_1im]Cl$; ∗, $[C_{14}C_1im]Cl$; and Δ, $[C_4C_1C_1im]Cl$. (Bottom) Correlated data in triangular diagrams (weight fraction units).

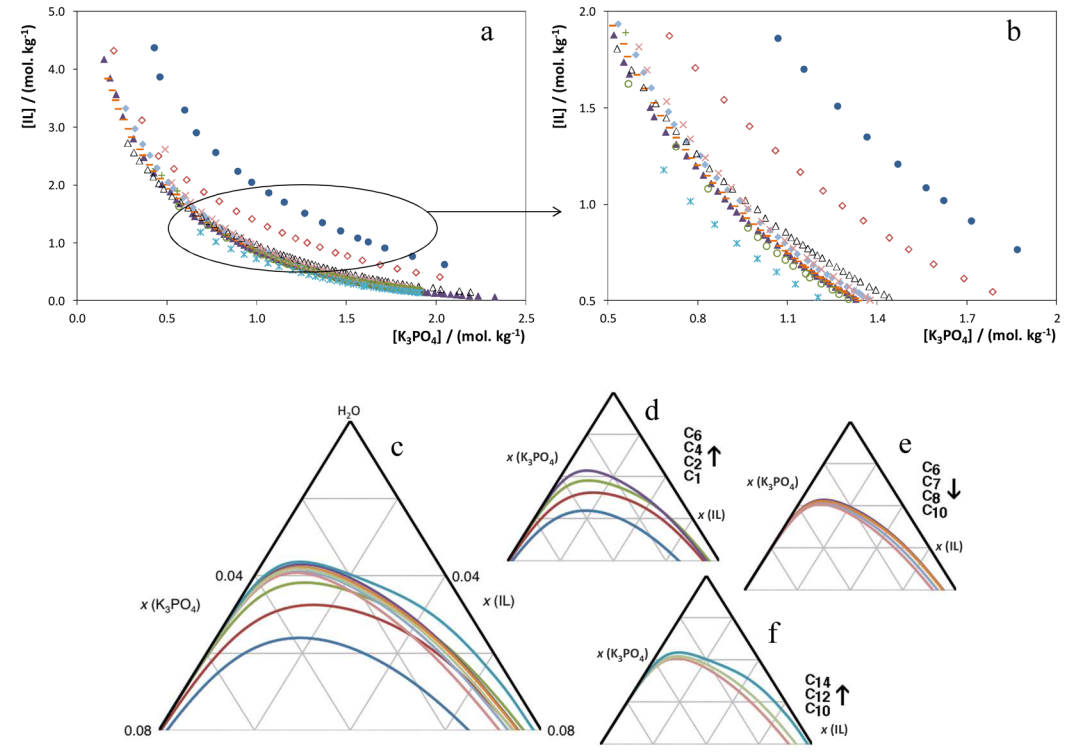

Figure 3. Ternary phase diagrams for K_3PO_4 + water + chloride-based ILs at 298 K and atmospheric pressure. (Top) Experimental data points in orthogonal diagrams (molality units): ●, $[C_1C_1im]Cl$; ◊, $[C_2C_1im]Cl$; +, $[C_4C_1im]Cl$; ▲, $[C_6C_1im]Cl$; -, $[C_7C_1im]Cl$; ♦, $[C_8C_1im]Cl$; ×, $[C_{10}C_1im]Cl$; ○, $[C_{12}C_1im]Cl$; ∗, $[C_{14}C_1im]Cl$; and Δ, $[C_4C_1C_1im]Cl$. (Bottom) Correlated data in triangular diagrams (mole fraction units).

system composition by the lever-arm rule,[31] for which the following system of four equations (eqs 2−5) and four unknown values ($[IL]_T$, $[IL]_B$, $[K_3PO_4]_T$, and $[K_3PO_4]_B$) was solved:

$$[IL]_T = A \exp[(B \times [K_3PO_4]_T^{0.5}) - (C \times [K_3PO_4]_T^3)] \quad (2)$$

dx.doi.org/10.1021/jp211132z | J. Phys. Chem. B 2012, 116, 7660−7668

Table 1. Parameters (A, B, and C) of Equation 1 for the Ternary Systems Composed of IL + K_3PO_4 + H_2O at 298 K and the Respective Standard Deviation (σ)

IL	$A \pm \sigma$	$B \pm \sigma$	10^5 ($C \pm \sigma$)	R^2
$[C_1C_1im]Cl$	109.9 ± 7.6	−0.374 ± 0.022	1.99 ± 0.33	0.9959
$[C_2C_1im]Cl$	75.4 ± 1.8	−0.330 ± 0.009	2.75 ± 0.16	0.9985
$[C_4C_1im]Cl$	70.3 ± 1.8	−0.302 ± 0.008	4.36 ± 0.10	0.9996
$[C_6C_1im]Cl$	83.6 ± 0.5	−0.334 ± 0.002	6.08 ± 0.05	0.9996
$[C_7C_1im]Cl$	84.3 ± 0.4	−0.320 ± 0.002	5.90 ± 0.04	0.9997
$[C_8C_1im]Cl$	97.8 ± 0.8	−0.342 ± 0.003	5.30 ± 0.05	0.9998
$[C_{10}C_1im]Cl$	107.4 ± 1.4	−0.338 ± 0.004	5.38 ± 0.04	0.9999
$[C_{12}C_1im]Cl$	94.9 ± 1.7	−0.309 ± 0.005	5.62 ± 0.05	0.9998
$[C_{14}C_1im]Cl$	72.0 ± 3.8	−0.238 ± 0.015	6.73 ± 0.14	0.9995
$[C_4C_1C_1im]Cl$	69.9 ± 0.4	−0.301 ± 0.002	4.74 ± 0.03	0.9999

$$[IL]_B = A \exp[(B \times [K_3PO_4]_B^{0.5}) - (C \times [K_3PO_4]_B^3)] \quad (3)$$

$$[IL]_T = \frac{[IL]_M}{\alpha} - \frac{1-\alpha}{\alpha} \times [IL]_B \quad (4)$$

$$[K_3PO_4]_T = \frac{[K_3PO_4]_M}{\alpha} - \frac{1-\alpha}{\alpha} \times [K_3PO_4]_B \quad (5)$$

where T, B, and M designate the top phase, the bottom phase and the mixture, respectively, $[K_3PO_4]$ and $[IL]$ represent the weight fraction percentage of the inorganic salt and IL, and α is the ratio between the mass of the top phase and the total mass of the mixture. The system solution results in the weight fraction percentage of the IL and inorganic salt in the top and bottom phases and, thus, represents the TLs of each system. For all of the systems investigated, the top phase corresponds to the IL-rich phase, whereas the bottom phase is the K_3PO_4-rich phase.

The tie-line length (TLL) and the tie-line slope (TLS) were determined using eqs 6 and 7, respectively.

$$TLL = \sqrt{([K_3PO_4]_T - [K_3PO_4]_B)^2 + ([IL]_T - [IL]_B)^2} \quad (6)$$

$$TLS = \frac{[IL]_T - [IL]_B}{[K_3PO_4]_T - [K_3PO_4]_B} \quad (7)$$

where T and B define, respectively, the top and bottom phases and $[K_3PO_4]$ and $[IL]$ are the weight fraction percentages of the solutes, as previously described.

The critical point of each system (the mixture composition at which the composition of the two aqueous phases becomes identical) was also estimated. The critical point was estimated by applying the Sherwood method and making use of the TL slopes.[32]

RESULTS AND DISCUSSION

Phase Diagrams. Because both the IL and the inorganic salt are composed of ions, it could be expected that ion exchange and differentiated ionic partition coefficients would lead to complex speciation within the equilibrated aqueous phases. Nevertheless, Bridges et al.[4] have shown that the ions' migration in the coexisting phases of the ABS composed of $[C_4C_1im]Cl$ + K_3PO_4 is not significant to yield inaccurate results on the concentration of each salt at both aqueous phases, taking into account the uncertainty already associated with the experimental procedure.

The experimental phase diagrams obtained at 298 K and atmospheric pressure for the ternary systems composed of inorganic salt + water + IL are depicted in Figures 2 and 3. The general overview of all of the ternary phase diagrams is presented in both weight fraction and molality units, in orthogonal and triangular representations, and in total and partial experimental sets to allow for further comparison. The experimental weight fraction data for each phase diagram are reported in the Supporting Information.

Table 1 presents the parameters of eq 1 obtained by the nonlinear regression of the experimental phase diagrams (in weight fraction percentages), as well as the corresponding correlation coefficients and associated standard deviations. As can be seen by the correlation coefficients (R^2) obtained, eq 1 provides a good description of the experimental binodal curves.

The TLs, TLLs, and TLSs for each system were determined through the application of eqs 2−7 and are reported in Table 2. An example of the TLs obtained in this work is depicted in Figure 4 for the system composed of $[C_8C_1im]Cl$. The TLs' data were further correlated by means of the Othmer−Tobias and Bancroft equations;[33,34] results shown in Supporting Information. The enhanced correlation coefficients obtained support the consistency and reliability of the TLs experimentally determined and the liquid−liquid equilibrium between two phases that are partially miscible in a ternary system. The graphical representation of the TLs for the remaining systems is also provided in the Supporting Information.

The critical point of each ternary system is presented in Table 3. As an example, the locus of the estimated critical point for the system composed of $[C_8C_1im]Cl$, K_3PO_4, and water is illustrated in Figure 4. The critical points of the remaining systems are depicted in the Supporting Information.

When an electrolyte is added to an aqueous solution containing another electrolyte (or even to a nonelectrolyte), the solubility of the solute in water decreases (or increases) depending on the salting-out (-in) aptitude of the ionic species. In the mixtures studied, which contain a high charge density salt (K_3PO_4) with an enhanced capacity for creating hydration complexes,[35,36] the capability for liquid−liquid demixing usually increases with the decrease in the IL's affinity for water since the IL is salted-out by the K_3PO_4 inorganic ions. The salting-out effect can be accounted for in terms of the complex and competing nature of interactions between the ions (IL and inorganic salt) and water. High charge density ions, such as those of the inorganic salt, are entropically favored to be hydrated in solution rather than the low charge density ions of the IL, leading, therefore, to an effective preferential exclusion

dx.doi.org/10.1021/jp211132z | J. Phys. Chem. B 2012, 116, 7660−7668

Table 2. Weight Fraction Compositions (wt %) for the Top (T) Phase, the Initial Mixture (M), and the Bottom (B) Phase of the Ternary Systems Composed of IL + K_3PO_4 + H_2O Systems at 298 K and the Respective Values for the Tie-Line Length (TLL) and Tie-Line Slope (TLS)

	weight fraction composition/wt %							
IL	$[IL]_T$	$[K_3PO_4]_T$	$[IL]_M$	$[K_3PO_4]_M$	$[IL]_B$	$[K_3PO_4]_B$	TLS	TLL
$[C_1C_1im]Cl$	36.20	8.634	10.25	29.90	6.106	33.30	−1.220	38.92
	45.98	5.402	10.02	31.85	4.758	35.72	−1.360	51.17
	57.60	2.985	10.11	33.90	3.639	38.12	−1.536	64.39
	68.80	1.571	10.08	36.11	2.748	40.42	−1.700	76.63
	72.42	1.246	10.03	37.92	2.058	42.61	−1.701	81.62
$[C_2C_1im]Cl$	31.56	6.850	24.82	13.27	4.331	32.80	−1.049	37.61
	35.80	5.064	25.29	14.78	3.233	35.16	−1.082	44.35
	37.79	4.369	26.30	14.93	2.638	36.68	−1.088	47.75
	43.06	2.887	24.64	19.00	1.918	38.89	−1.143	54.67
	47.22	2.017	24.88	20.85	1.470	40.59	−1.186	59.84
$[C_4C_1im]Cl$	36.90	4.474	24.36	14.92	2.718	32.96	−1.200	44.49
	38.32	4.001	24.96	15.38	1.932	34.99	−1.174	47.79
	43.69	2.542	24.94	17.66	1.434	36.62	−1.240	54.28
	46.99	1.868	30.32	14.76	1.277	37.22	−1.293	57.79
	54.64	0.7997	34.99	15.48	0.5442	41.21	−1.339	67.52
$[C_6C_1im]Cl$	32.98	7.356	24.91	13.03	3.876	27.82	−1.422	35.58
	41.13	4.442	25.12	14.89	2.922	29.38	−1.532	45.63
	43.95	3.672	23.03	17.65	1.780	31.85	−1.497	50.72
	50.06	2.353	25.16	18.14	1.293	33.28	−1.578	57.75
	54.36	1.661	25.00	20.07	0.8011	35.25	−1.594	63.22
$[C_7C_1im]Cl$	37.00	6.395	25.18	14.10	4.608	27.52	−1.533	38.68
	42.36	4.564	25.01	15.26	4.173	28.12	−1.621	44.87
	48.30	3.020	24.98	17.25	2.461	30.98	−1.639	53.70
	52.03	2.275	30.78	14.68	2.313	31.30	−1.713	57.57
	56.20	1.608	25.00	20.09	1.243	34.15	−1.689	63.87
$[C_8C_1im]Cl$	38.71	7.043	25.07	15.07	7.010	25.70	−1.699	36.78
	42.80	5.694	24.91	16.07	5.551	27.31	−1.723	43.06
	47.94	4.289	24.88	17.62	3.654	29.89	−1.730	51.16
	52.63	3.260	25.09	18.92	2.634	31.69	−1.758	57.52
	57.56	2.394	24.92	21.24	1.381	34.83	−1.732	64.87
$[C_{10}C_1im]Cl$	26.11	14.00	10.06	24.92	5.448	28.06	−1.470	24.99
	31.67	11.39	9.981	26.03	3.799	30.20	−1.481	33.63
	38.49	8.604	10.24	26.98	2.826	31.80	−1.537	42.54
	41.92	7.391	10.11	27.96	2.190	33.08	−1.547	47.31
	50.33	4.948	9.961	29.01	1.871	33.83	−1.678	56.41
$[C_{12}C_1im]Cl$	28.30	12.59	9.932	25.38	4.349	29.27	−1.434	29.19
	31.76	10.90	9.891	26.01	3.573	30.38	−1.447	34.26
	34.85	9.497	9.888	26.55	3.044	31.22	−1.464	38.52
	36.76	8.676	10.15	27.02	2.448	32.32	−1.451	41.68
$[C_{14}C_1im]Cl$	16.30	18.85	5.008	28.98	2.397	31.33	−1.115	18.68
	21.45	15.78	5.016	30.04	1.647	32.96	−1.153	26.21
	25.79	13.29	5.000	30.93	1.233	34.13	−1.179	32.31
	31.16	10.29	5.009	32.01	0.8698	35.45	−1.204	39.37
$[C_4C_1C_1im]Cl$	26.64	9.456	15.00	20.03	3.460	30.50	−1.101	31.31
	32.35	6.358	15.03	21.90	2.039	33.57	−1.114	40.73
	36.83	4.480	15.38	23.42	1.300	35.85	−1.133	47.40
	39.66	3.525	15.32	25.01	0.8569	37.77	−1.133	51.75
	44.48	2.254	15.10	27.07	0.5928	39.33	−1.184	57.45

and to the two-phase formation.[35,36] In summary, the salting-out effect is mainly the result of the formation of water−ion complexes that cause the dehydration of the solute and increase the surface tension of the cavity in aqueous media.[35,36]

In general, ILs with lower affinities for water require less salt to induce the separation of the two aqueous phases, resulting in a binodal curve closer to the axis and to a larger biphasic region. The diagrams depicted in Figures 2 and 3 show that such a simplistic approach does not hold for the entire IL homologous series studied in this work. From Figure 2, the IL aptitude for forming a second liquid phase, for instance, at ∼18 wt % of K_3PO_4, follows the rank $[C_1C_1im]Cl < [C_{10}C_1im]Cl \approx [C_{12}C_1im]Cl \approx [C_{14}C_1im]Cl < [C_8C_1im]Cl < [C_2C_1im]Cl < [C_7C_1im]Cl < [C_4C_1C_1im]Cl \approx [C_4C_1im]Cl < [C_6C_1im]Cl$. Using this type of representation, a direct correlation of the ILs' aptitude for salting-out is not easily assessed. Weight fraction

dx.doi.org/10.1021/jp211132z | J. Phys. Chem. B 2012, 116, 7660−7668

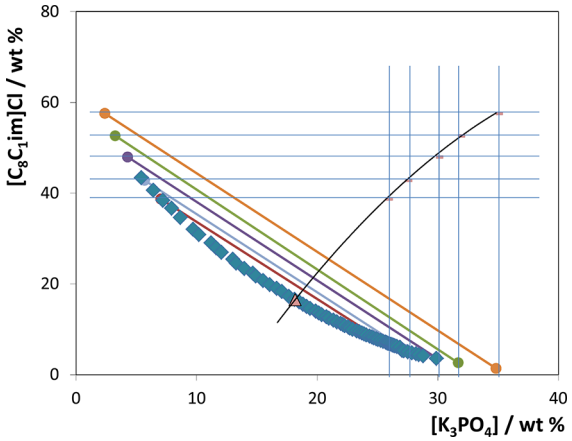

Figure 4. Binodal curve (♦), TLs (●), and critical point (▲) estimated by the Sherwood method[32] for the system composed of $[C_8C_1im]Cl + K_3PO_4 + H_2O$ at 298 K.

Table 3. Critical Point for Each System Composed of IL + K_3PO_4 + H_2O at 298 K and Correlation Coefficients of the Polynomial Fittings (R^2)

		critical point/wt %		
IL	R^2	[IL]	$[K_3PO_4]$	$[H_2O]$
$[C_1C_1im]Cl$	0.9901	9.141	28.88	61.98
$[C_2C_1im]Cl$	0.9979	9.862	24.49	65.65
$[C_4C_1im]Cl$	0.9621	13.82	18.90	67.28
$[C_6C_1im]Cl$	0.9748	6.222	24.85	68.93
$[C_7C_1im]Cl$	0.9721	6.468	25.34	68.19
$[C_8C_1im]Cl$	0.9975	16.54	18.17	65.29
$[C_{10}C_1im]Cl$	0.9824	7.856	25.61	66.54
$[C_{12}C_1im]Cl$	0.9938	7.928	25.42	66.65
$[C_{14}C_1im]Cl$	1.0000	6.260	26.28	67.46
$[C_4C_1C_1im]Cl$	0.9938	13.21	19.35	67.44

units can indeed be misleading due to the molecular weight differences of the various ILs. Using molality units, the differences that could be the mere result of different molecular weights of ILs are avoided, allowing for a more comprehensive analysis of the effect of individual solutes on promoting the liquid−liquid demixing, as shown in Figure 3. Here, the binodal curves represented in molality units illustrate that the ILs' ability for ABS formation at 1.0 mol·kg^{-1} of K_3PO_4 follows the order $[C_1C_1im]Cl < [C_2C_1im]Cl < [C_4C_1im]Cl < [C_4C_1C_1im]Cl < [C_{10}C_1im]Cl \approx [C_8C_1im]Cl < [C_7C_1im]Cl \approx [C_6C_1im]Cl < [C_{12}C_1im]Cl < [C_{14}C_1im]Cl$. A somewhat more logical and clearer trend is thus observed as far as the smaller ILs are concerned, but it is still not monotonous within the entire homologous series. We have previously observed[8] that an increase in the cation alkyl chain length of the IL leads to an improved ability for phase separation due to the increase of the fluids' overall hydrophobicity and lower affinity for water.[37] The recent ABS data[8] for systems comprised of the $[C_nC_1im]Cl$ (n = 1−6) ILs are in close agreement with the present results, including the trends depicted in Figures 2d and 3d. On the other hand, another report[5] describing ABS formation in systems with $[C_nC_1im]Cl$, with n = 4, 8, and 10, has shown that the locus of the homogeneous region increases as the alkyl side-chain length increases. The comparisons between this latter (fragmented) series[5] and the present work are also favorable.

The point to be made at this stage is that the ABS formation along a series of homologous ILs (when increasing the alkyl side-chain length) is a complex affair, and the use of just a few members of the series does not allow a full analysis of the effect. Figures 2d−f and 3d−f show that there are different trends on the ABS formation along the studied homologous IL series. Therefore, because the salting-out species is always common (K_3PO_4), the two-phase forming ability is a main result of the salting-in aptitude of each IL. In this respect, we decided here to examine the salting-out effects of the phosphate salt toward each IL aqueous solution by means of a quantitative salting-out coefficient.

Salting-out effects are usually quantified by the fitting of solubility data to the empirical equation of Setschenow and according to[38]

$$\ln \frac{S_0}{S} = k_s c_s \tag{8}$$

where S_0 and S correspond to the solubility of a given solute in pure water and in a salt solution, respectively, and c_s is the concentration of salt. k_s is defined as the salting-out coefficient or Setschenow constant for a particular solute−salt pair.

In older studies, the Setschenow-type behavior of phase diagrams composed of polymers and salts has been ascertained by some authors[39,40] but with limited success. As a result, Hey et al.[41] proposed a new derivation for eq 8, which was shown to be successful in the description of polymer-based ABS and later on in the description of IL-salt-based ABS by Zafarani-Moattar and Hamzehzadeh.[10,42] The proposed equation is described as follows

$$\ln \frac{[IL]_T}{[IL]_B} = k_{IL}([IL]_B - [IL]_T) + k_s([K_3PO_4]_B - [K_3PO_4]_T) \tag{9}$$

where [IL] and $[K_3PO_4]$ represent the molality of IL and K_3PO_4, T and B designate the top and bottom phases, respectively, and k_{IL} and k_s are a parameter relating the activity coefficient of the IL to its concentration and the salting-out coefficient, respectively.

Zafarani-Moattar and Hamzehzadeh[10,42] showed that eq 9, typically applied to the nonelectrolyte−salt ABS, satisfactorily describes IL salt systems because ILs display remarkable hydrophobic associations in aqueous solution (contrarily to high charge density salts).[43,44]

The salting-out coefficient derived from eq 9 is related to the extent of the preferential hydration of the salt and thus to the poorer hydration of each IL. Therefore, from the TL compositions described in Table 2 and respective conversion to molality units (cf. Supporting Information), we fitted the logarithm of the ratio between the molality of the IL in the top phase to the one in the bottom phase as a linear function of the difference between the molality of K_3PO_4 in the bottom phase to that in the top phase. The Setschenow-type plots obtained are depicted in the Supporting Information. The slopes from the fitting by eq 9 give the salting-out coefficients. The k_s values, the corresponding intercepts, and correlation coefficients are presented in Table 4. On the basis of the correlation coefficients obtained, it is possible to conclude that the equilibrium compositions of the investigated systems can be satisfactorily characterized by a Setschenow-type behavior.

When representing the quantitative salting-out coefficients, k_s, as a function of the size of the alkyl chain in $[C_nC_1im]Cl$,

dx.doi.org/10.1021/jp211132z | J. Phys. Chem. B 2012, 116, 7660−7668

Table 4. Parameters Obtained from the Fitting of the Setschenow-Type Behavior (eq 9) and the Respective Correlation Coefficients (R^2)

IL	k_s/(kg·mol^{-1})	$k_{IL}([IL]_B - [IL]_T)$	R^2
$[C_1C_1im]Cl$	1.7831	−1.2861	0.9966
$[C_2C_1im]Cl$	1.5171	−0.6696	0.9985
$[C_4C_1im]Cl$	2.0343	−1.2715	0.9982
$[C_6C_1im]Cl$	2.3837	−0.9832	0.9973
$[C_7C_1im]Cl$	2.3640	−0.9928	0.9988
$[C_8C_1im]Cl$	2.1707	−0.6715	0.9989
$[C_{10}C_1im]Cl$	1.9566	−0.3184	0.9972
$[C_{12}C_1im]Cl$	1.8435	−0.1885	0.9996
$[C_{14}C_1im]Cl$	1.8871	0.0834	1.0000
$[C_4C_1C_1im]Cl$	1.8781	−0.6933	0.9974

three patterns are clearly identifiable, Figure 5. Taking into account the k_s values, the IL is increasingly able to form ABS as

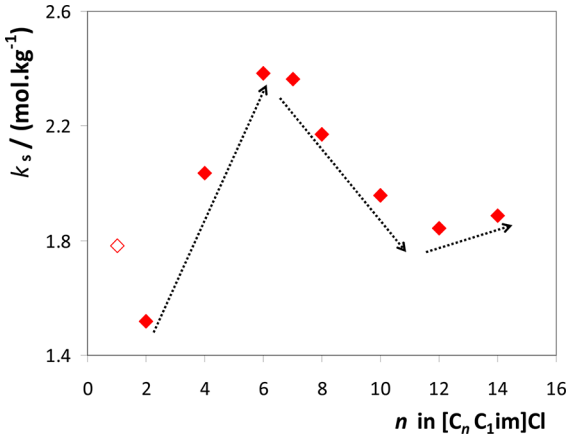

Figure 5. Salting-out coefficients (k_s) (♦) as a function of the alkyl chain length, n, in $[C_nC_1im]Cl$ ILs. The symbol ◊ represents the k_s value for $[C_1C_1im]Cl$.

the alkyl side chain grows from $[C_2C_1im]Cl$ to $[C_6C_1im]Cl$, while from $[C_6C_1im]Cl$ to $[C_{12}C_1im]Cl$, the opposite behavior is observed. From $[C_{12}C_1im]Cl$ to $[C_{14}C_1im]Cl$, again, the likeliness of the IL to undergo liquid−liquid demixing is enhanced as the alkyl chain lengthens, albeit in a slightly pronounced way. $[C_1C_1im]Cl$ can be identified however as an outlier regarding the first trend. We think that this fact is due to the high charge density of $[C_1C_1im]^+$ when compared with the homologous series with longer aliphatic chains.

When moving from $[C_2C_1im]Cl$ to $[C_6C_1im]Cl$, the trend observed is a direct outcome of solvophobic and entropic effects; increasing the alkyl side-chain length of the IL cation enhances the fluid's overall hydrophobicity while decreasing the entropy of the solution.[45] Hence, the phase separation is facilitated by ILs with longer aliphatic chains. From $[C_6C_1im]Cl$ onward, a trend shift occurs. This can be rationalized in terms of a larger degree of self-aggregation of the ILs in water. Self-aggregation does not exist for systems containing ILs with alkyl chains shorter than the hexyl, but it has been shown to occur in aqueous solutions of $[C_nC_1im]Cl$, with $n > 6$, above the corresponding critical micelle concentration (CMC).[27] Furthermore, it is well-known that the presence of salting-out-inducing salts decreases the CMC and facilitates the aggregation of ILs, a phenomenon attributed to the reduction of the repulsion between the imidazolium head groups due to the presence of higher concentrations of counterions.[27] Yet, if the formation of ABS were dominated by micelle formation, the trend observed after $[C_6C_1im]Cl$ should be straightforwardly maintained until $[C_{14}C_1im]Cl$ because the CMC of this series of chloride-based ILs decreases progressively from 900 to 4 mM.[27] On the other hand, if the size of the ionic fluids was the dominant effect, the rank on the ILs would be direct because there is a rise in the molar volume of the IL with the increase of the cation side alkyl chain length from $[C_2C_1im]^+$ to $[C_{14}C_1im]^+$.[46] The complex behavior presented in Figure 5 suggests that, for ILs above $[C_6C_1im]Cl$, there is a dominant effect of the IL to self-aggregate in aqueous media, reflected by the lower k_s values, which further indicate a lower ability for liquid−liquid demixing. Nevertheless, the slight inversion of behavior observed after $[C_{12}C_1im]Cl$ points to a delicate balance between these two competing effects, the entropic contributions that decrease the solubility of ILs in water and their tendency to self-aggregate in aqueous media.

It should be pointed out that experimental and simulation results demonstrated that the self-aggregation of ILs is not strictly limited for their dissolution in water. Yet, it occurs even in neat ILs.[24,47] We recently observed similar trend changes for other thermophysical and transport properties of neat ILs, such as their enthalpies and entropies of vaporization and viscosities.[47,48] The nanosegregation observed in neat ILs is not only responsible for trend shifts in their pure state properties but also has an impact in the phase behavior of more complex systems, for instance, in the ternary phase diagrams studied in this work.

In polymer-salt-based ABS,[49] the salt anion has a major impact on the behavior of the phase diagrams, whereas the cation has a minor (yet sizable) influence. This fact is a direct result of the higher aptitude of anions to be hydrated because they are more polarizable than cations due to their more diffuse valence electronic configuration (other ad hoc facts also help for this state of affairs; most inorganic anions are molecular species, whereas the cations are atomic; some of the most commonly used anions are di- or trivalent, whereas most cations are mono- or divalent).[35,36] As a result, salting-in/-out effects are more pronounced when different anions are compared.[36] The hydrogen-bonding ability of ILs can be empirically estimated using a variety of solvatochromic probes, designed to measure only a single interaction (hydrogen-bonding), as previously described in the literature.[50,51] One of most widely used set of solvatochromic parameters are the Kamlet−Taft parameters. They embrace the solvent dipolarity/polarizability (π^*), the hydrogen-bond acidity (α), and the hydrogen-bond basicity (β).[51] The β-scale is a measure of the ability of the solvent to accept a proton (or donate an electron pair) in a solute−solvent hydrogen bond, while the α-scale defines the hydrogen-bond donation ability of the solute. The α value is largely determined by the availability of hydrogen-bond donor sites at the imidazolium cation, while the β parameter is mainly ruled by the IL anion. We have previously demonstrated that the ability of the IL anion to promote phase separation is closely related to its ability to hydrogen bond with water.[9] IL anions with a lower hydrogen-bond acceptor strength (lower hydrogen-bond basicity values) are more able to undergo liquid−liquid demixing.[9] On the other hand, the acidity of the proton attached to the carbon in position 2 on the imidazolium ring is the main factor responsible for the α values representing the ability of the cation to hydrogen bond with water. Values of α taken from the literature[52] ($[C_4C_1im]Cl$ = 0.32, $[C_6C_1im]Cl$

dx.doi.org/10.1021/jp211132z | J. Phys. Chem. B 2012, 116, 7660−7668

= 0.31, $[C_8C_1im]Cl$ = 0.31, and $[C_{10}C_1im]Cl$ = 0.31) indicate that, above $[C_6C_1im]Cl$, the ability of the cation to hydrogen bond with water is nearly identical. Therefore, on the basis of the trend shifts shown in Figure 3, the influence of the IL cation to form ABS is mainly dominated by entropic contributions and stereochemical effects and not by their hydrogen-bonding ability with water, when a homologous series of the type $[C_nC_1im]Cl$ is considered. Moroever, the k_s value for the system composed of $[C_4C_1C_1im]Cl$ (Table 4) is lower than that expected (if a structural isomer of the type $[C_5C_1im]Cl$ is visualized), meaning that the ability of this IL to undergo liquid−liquid demixing is consequently lower. It is well-accepted that the substitution of the most acidic hydrogen at C2 by an alkyl group largely reduces the ability of the IL to hydrogen bond. Hence, this result supports the idea that if the hydrogen bonding of the IL cation with water would be important, $[C_4C_1C_1im]Cl$ would be more easily phase separated than it really is.

Previous data on the mutual solubilities of hydrophobic ILs and water[45,53,54] can be used to support the above conclusions. For 1-alkyl-3-methylimidazolium-based ILs, the increase of the alkyl chain length decreases the mutual solubilities between water and ILs.[45] The decrease of the ILs' solubility in water is driven by a decrease in the entropy of solution (for structurally similar ILs).[45] On the other hand, anion−water interactions are more important in defining the mutual solubilities, and in addition to the entropic contribution, changes in the enthalpy of solution are also observed.[53] In fact, it is the anion solvation at the IL-rich phase that controls the solubility of ILs in water.[53] The introduction of an alkyl group at the C2 position on the imidazolium ring, $[C_4C_1C_1im]^+$, has two different consequences; it leads to a strong decrease in the water solubility in ILs whereas the solubility of the IL in water is similar to the structural analogue $[C_5mim]^+$.[53] This suggests that hydrogen bonding with water is more relevant at the IL-rich phase while the ionic fluid solvation in water is more dependent on the cation size.[53,54] The phase behavior observed for the binary mixtures previously studied[45,53,54] can thus be extended to explain the behavior of the ternary systems studied in this work. The behavior of the phase diagrams of ABS composed of ILs with different anions correlates well with the solute−water hydrogen-bonding capacity, whereas for ABS with diverse cations, the phenomenon depends on a combined effect regarding mainly the size of the cation and their aptitude for self-aggregation in aqueous media.

CONCLUSIONS

Aiming at confirming different patterns previously observed in the literature on IL-based ABS, this work reports, for the first time, an extensive analysis of the effect of the alkyl side-chain length of the cation and the influence of the substitution of the most acidic hydrogen at the imidazolium core by a methyl group. The results indicate that the lengthening of the cation alkyl chain leads to an improved ability for phase separation if ILs of the type $[C_nC_1im]Cl$, with n = 1−6, are considered. Nevertheless, for longer alkyl side chains, a more complex ratio between entropic contributions and the ability of each IL to self-aggregate in aqueous media control the phase behavior. The trend shifts observed in the phase diagram's behavior were supported by the Setschenow-type salting-out coefficients, which reflect the extent of the preferential hydration of each IL. The introduction of an alkyl group at the C2 position on the imidazolium ring, $[C_4C_1C_1im]^+$, allowed us to conclude that the hydrogen bonding between the IL cation and water is not a determinant effect toward the formation of ABS.

ASSOCIATED CONTENT

Supporting Information

Experimental weight fraction data for the solubility curves, correlation of the TL compositions ascertained by the Othmer−Tobias and Bancroft correlations, representation of the TLs and critical points, TL compositions in molality units, and Setschenow-type plots. This material is available free of charge via the Internet at http://pubs.acs.org.

AUTHOR INFORMATION

Corresponding Author

*E-mail: maragfreire@ua.pt (M.G.F.); luis.rebelo@itqb.unl.pt (L.P.N.R.).

Notes

The authors declare no competing financial interest.

ACKNOWLEDGMENTS

This work was financed by national funding from FCT, Fundação para a Ciência e a Tecnologia, through the Projects PTDC/QUI-QUI/121520/2010 and Pest-C/CTM/LA0011/2011. The authors also acknowledge FCT for the postdoctoral and doctoral Grants SFRH/BPD/41781/2007 and SFRH/BD/70641/2010 of M.G.F. and C.M.S.S.N., respectively.

REFERENCES

(1) Albertsson, P. A. *Partitioning of Cell Particles and Macromolecules*, 3rd ed.; Wiley: New York, 1986.
(2) Banik, R. M.; Santhiagu, A.; Kanari, B.; Sabarinath, C.; Upadhyay, S. N. *World J. Microbiol. Biotechnol.* **2003**, *19*, 337−348.
(3) Gutowski, K. E.; Broker, G. A.; Willauer, H. D.; Huddleston, J. G.; Swatloski, R. P.; Holbrey, J. D.; Rogers, R. D. *J. Am. Chem. Soc.* **2003**, *125*, 6632−6633.
(4) Bridges, N. J.; Gutowski, K. E.; Rogers, R. D. *Green Chem.* **2007**, *9*, 177−183.
(5) Najdanovic-Visak, V.; Canongia Lopes, J. N.; Visak, Z. P.; Trindade, J.; Rebelo, L. P. N. *Int. J. Mol. Sci.* **2007**, *8*, 736−748.
(6) Canongia Lopes, J. N.; Rebelo, L. P. N. *Chim. Oggi* **2007**, *25*, 37−39.
(7) Zafarani-Moattar, M. T.; Hamzehzadeh, S. *J. Chem. Eng. Data* **2007**, *52*, 1686−1692.
(8) Neves, C. M. S. S.; Ventura, S. P. M.; Freire, M. G.; Marrucho, I. M.; Coutinho, J. A. P. *J. Phys. Chem. B* **2009**, *113*, 5194−5199.
(9) Ventura, S. P. M.; Neves, C. M. S. S.; Freire, M. G.; Marrucho, I. M.; Oliveira, J.; Coutinho, J. A. P. *J. Phys. Chem. B* **2009**, *113*, 9304−9310.
(10) Zafarani-Moattar, M. T.; Hamzehzadeh, S. *J. Chem. Eng. Data* **2009**, *54*, 833−841.
(11) Louros, C. L. S.; Cláudio, A. F. M.; Neves, C. M. S. S.; Freire, M. G.; Marrucho, I. M.; Pauly, J.; Coutinho, J. A. P. *Int. J. Mol. Sci.* **2010**, *11*, 1777−1791.
(12) Cláudio, A. F. M.; Ferreira, A. M.; Shahriari, S.; Freire, M. G.; Coutinho, J. A. P. *J. Phys. Chem. B* **2011**, *115*, 11145−11153.
(13) Deive, F. J.; Rodríguez, A.; Marrucho, I. M.; Rebelo, L. P. N. *J. Chem. Thermodyn.* **2011**, *43*, 1565−1572.
(14) Zhang, Y.; Zhang, S.; Chen, Y.; Zhang, J. *Fluid Phase Equilib.* **2007**, *257*, 173−179.
(15) Wu, B.; Zhang, Y.; Wang, H.; Yang, L. *J. Phys. Chem. B* **2008**, *112*, 13163−13165.
(16) Freire, M. G.; Louros, C. L. S.; Rebelo, L. P. N.; Coutinho, J. A. P. *Green Chem.* **2011**, *13*, 1536−1545.
(17) Zhang, J.; Zhang, Y.; Chen, Y.; Zhang, S. *J. Chem. Eng. Data* **2007**, *52*, 2488−2490.

(18) Domínguez-Pérez, M.; Tomé, L. I. N.; Freire, M. G.; Marrucho, I. M.; Cabeza, O.; Coutinho, J. A. P. *Sep. Purif. Technol.* **2010**, *72*, 85−91.
(19) Wei, X.-L.; Wei, Z.-B.; Wang, X.-H.; Wang, Z.-N.; Sun, D.-Z.; Liu, J.; Zhao, H. H. *Soft Matter* **2011**, *7*, 5200−5207.
(20) Freire, M. G.; Cláudio, A. F. M.; Araújo, J. M. M.; Coutinho, J. A. P.; Marrucho, I. M.; Canongia Lopes, J. N.; Rebelo, L. P. N. *Chem. Soc. Rev.* **2012**, DOI: 10.1039/C2CS35151J.
(21) Earle, M. J.; Esperança, J. M. S. S.; Gilea, M. A.; Canongia Lopes, J. N.; Rebelo, L. P. N.; Magee, J. W.; Seddon, K. R.; Widegren, J. A. *Nature* **2006**, *439*, 831−834.
(22) Santos, L. M. N. B. F.; Canongia Lopes, J. N.; Coutinho, J. A. P.; Esperança, J. M. S. S.; Gomes, L. R.; Marrucho, I. M.; Rebelo, L. P. N. *J. Am. Chem. Soc.* **2007**, *129*, 284−285.
(23) Pereira, J. F. B.; Lima, A. S.; Freire, M. G.; Coutinho, J. A. P. *Green Chem.* **2010**, *12*, 1661−1669.
(24) Canongia Lopes, J. N.; Pádua, A. A. *J. Phys. Chem. B* **2006**, *110*, 3330−3335.
(25) Blesic, M.; Lopes, A.; Melo, E.; Petrovski, Z.; Plechkova, N. V.; Canongia Lopes, J. N.; Seddon, K. R.; Rebelo, L. P. N. *J. Phys. Chem. B* **2008**, *112*, 8645−8650.
(26) Shimizu, K.; Tariq, M.; Costa Gomes, M. F.; Rebelo, L. P. N.; Canongia Lopes, J. N. *J. Phys. Chem. B* **2010**, *114*, 5831−5834.
(27) Blesic, M.; Marques, M. H.; Plechkova, N. V.; Seddon, K. R.; Rebelo, L. P. N.; Lopes, A. *Green Chem.* **2007**, *9*, 481−490.
(28) Deng., Y.; Chen, J.; Zhang, D. *J. Chem. Eng. Data* **2007**, *52*, 1332−1335.
(29) Pei, Y.; Wang, J.; Liu, L.; Wu, K.; Zhao, Y. *J. Chem. Eng. Data* **2007**, *52*, 2026−2031.
(30) Pei, Y.; Wang, J.; Wu, K.; Xuan, X.; Lu, X. *Sep. Purif. Technol.* **2009**, *64*, 288−295.
(31) Merchuk, J. C.; Andrews, B. A.; Asenjo, J. A. *J. Chromatogr., B* **1998**, *711*, 285−293.
(32) Seader, J. D.; Henley, E. J. *Separation Process Principles*, 2nd ed.; John Wiley & Sons: New York, 2006.
(33) Othmer, D. F.; Tobias, P. E. *Ind. Eng. Chem.* **1942**, *34*, 693−696.
(34) González-Tello, P.; Camacho, F.; Blázquez, G.; Alarcón, F. J. *J. Chem. Eng. Data* **1996**, *41*, 1333−1336.
(35) Freire, M. G.; Carvalho, P. J.; Silva, A. M. S.; Santos, L. M. N. B. F.; Rebelo, L. P. N.; Marrucho, I. M.; Coutinho, J. A. P. *J. Phys. Chem. B* **2009**, *113*, 202−211.
(36) Freire, M. G.; Neves, C. M. S. S.; Silva, A. M. S.; Santos, L. M. N. B. F.; Marrucho, I. M.; Rebelo, L. P. N.; Shah, J. K.; Maginn, E. J.; Coutinho, J. A. P. *J. Phys. Chem. B* **2010**, *114*, 2004−2014.
(37) Fernandes, A. M.; Rocha, M. A. A.; Freire, M. G.; Marrucho, I. M.; Coutinho, J. A. P.; Santos, L. M. N. B. F. *J. Phys. Chem. B* **2011**, *115*, 4033−4041.
(38) Setschenow, J. *Z. Phys. Chem.* **1889**, *4*, 117−125.
(39) Ananthapadmanabhan, K. P.; Goddard, E. D. *Langmuir* **1987**, *3*, 25−21.
(40) Zaslavsky, B. Y.; Gulaeva, N. D.; Djafarov, S.; Masimov, E. A.; Miheeva, L. M. *J. Colloid Interface Sci.* **1990**, *137*, 147−156.
(41) Hey, M. J.; Jackson, D. P.; Yan, H. *Polymer* **2005**, *46*, 2567−2572.
(42) Zafarani-Moattar, M. T.; Hamzehzadeh, S. *J. Chem. Eng. Data* **2010**, *55*, 1598−1610.
(43) Gardas, R. L.; Dagade, D. H.; Coutinho, J. A. P.; Patil, K. *J. Phys. Chem. B* **2008**, *112*, 3380−3389.
(44) Shekaari, H.; Mousavi, S. S. *J. Chem. Thermodyn.* **2009**, *41*, 90−96.
(45) Freire, M. G.; Carvalho, P. J.; Gardas, R. L.; Marrucho, I. M.; Santos, L. M. N. B. F.; Coutinho, J. A. P. *J. Phys. Chem. B* **2008**, *112*, 1604−1610.
(46) Tariq, M.; Serro, A. P.; Mata, J. L.; Saramago, B.; Esperança, J. M. S. S.; Canongia Lopes, J. N.; Rebelo, L. P. N. *Fluid Phase Equilib.* **2010**, *294*, 131−138.
(47) Rocha, M. A. A.; Lima, C. F. R. A. C.; Gomes, L. R.; Schröder, B.; Coutinho, J. A. P.; Marrucho, I. M.; Esperança, J. M. S. S.; Rebelo, L. P. N.; Shimizu, K.; Canongia Lopes, J. N.; Santos, L. M. N. B. F. *J. Phys. Chem. B* **2011**, *115*, 10919−10926.
(48) Tariq, M.; Carvalho, P. J.; Coutinho, J. A. P.; Marrucho, I. M.; Canongia Lopes, J. N.; Rebelo, L. P. N. *Fluid Phase Equilib.* **2011**, *301*, 22−32.
(49) Rogers, R. D.; Bauer, C. B. *J. Chromatogr., B* **1996**, *680*, 237−241.
(50) Reichardt, C. *Green Chem.* **2005**, *7*, 339−351.
(51) Ab Rani, M. A.; Brant, A.; Crowhurst, L.; Dolan, A.; Lui, M.; Hassan, N. H.; Hallett, J. P.; Hunt, P. A.; Niedermeyer, H.; Perez-Arlandis, J. M.; Schrems, M.; Welton, T.; Wilding, R. *Phys. Chem. Chem. Phys.* **2011**, *13*, 16831−16840.
(52) Lungwitz, R.; Strehmel, V.; Spange, S. *New J. Chem.* **2010**, *34*, 1135−1140.
(53) Freire, M. G.; Neves, C. M. S. S.; Carvalho, P. J.; Gardas, R. L.; Fernandes, A. M.; Marrucho, I. M.; Santos, L. M. N. B. F.; Coutinho, J. A. P. *J. Phys. Chem. B* **2007**, *111*, 13082−13089.
(54) Freire, M. G.; Neves, M. S. S. S.; Shimizu, K.; Bernardes, C. E. S.; Marrucho, I. M.; Coutinho, J. A. P.; Canongia Lopes, J. N.; Rebelo, L. P. N. *J. Phys. Chem. B* **2011**, *114*, 15925−15934.